Hindawi
Journal of Chemistry
Volume 2020, Article ID 4926809, 10 pages
https://doi.org/10.1155/2020/4926809

*Research Article*

# Adsorption of Thymol onto Natural Clays of Morocco: Kinetic and Isotherm Studies

**Hamid Ziyat**,[1] **Mohammed Naciri Bennani**,[1] **Hassan Hajjaj**,[2] **Omar Qabaqous**,[1] **Said Arhzaf**,[1] **Soumiya Mekdad**,[1] **and Safae Allaoui**[1]

[1]*Laboratory of Chemistry-Biology Applied to the Environment, Research Team "Applied Materials and Catalyses" Chemistry Department, Faculty of Sciences, Moulay-Ismail University, BP. 11201 Zitoune, Meknes, Morocco*
[2]*Laboratory of Plant Biotechnology and Molecular Biology, Applied Mycology Team, Faculty of Sciences, Moulay-Ismail University, BP. 11201 Zitoune, Meknes, Morocco*

Correspondence should be addressed to Hamid Ziyat; ziyat.hamid@gmail.com

Received 1 July 2019; Revised 18 September 2019; Accepted 25 October 2019; Published 10 February 2020

Guest Editor: Yaowen Xing



The present work aims to study the affinity of a component of the thyme essential oil "thymol" to natural Moroccan clay "Rhassoul" using the adsorption technique. The physicochemical characterizations of the purified and modified clay were carried out by X-ray diffraction (XRD), Fourier transform infrared spectroscopy (FTIR), DTA/TGA, and SEM-EDX. Thymol adsorption tests on the purified Rhassoul (Rh-P) and the modified one by CTAB (Rh-CTAB) were followed by UV-visible spectroscopy. They show that the adsorption isotherms can be described by the Freundlich model and that the kinetics of adsorption is in accordance with the pseudo-second-order model for the two clays. Adsorption capacities obtained were of the order of 6 mg/g for the purified Rhassoul and 16 mg/g for the modified Rhassoul by cetyltrimethylammonium bromide (CTAB). These values show that the modified Rhassoul has a better adsorption capacity compared to the purified Rhassoul.

## 1. Introduction

Rhassoul is a natural clay soil of Moroccan origin, traditionally used for centuries in cosmetics (soap, shampoo, masks,...) by all the populations of North Africa and even in some regions of the Middle East. The Rhassoul deposits, unique in the world, are located on the edge of the southeast of the tertiary sector of Missour in the Moulouya valley 200 km from the Fes city. Rhassoul is a natural mineral product composed mainly of stevensite and other minerals such as quartz, gypsum, dolomite, or sepiolite but in low proportions [1]. The use of Rhassoul as an adsorbent is justified by its low cost, natural abundance, and high surface area. Rhassoul has been the subject of some recent studies which concerned the adsorption of fungicides [2], adsorption of textile dyes such as methylene blue [3, 4], basic yellow cationic dye [5], and methyl violet [6], and also other applications in water treatment [7–11].

The use of essential oils in antifungal applications for the preservation of foodstuffs is limited by the volatile nature of their constituents. Indeed, the essential oils are mainly formed of terpenoids that have high vaporization pressure at 25°C [12]. Because of the high volatility of essential oils or their constituents, the duration of their activities is very short. So, to increase their activities and to control their release, they can be encapsulated in clays or modified clays [13, 14]. The development of clay-essential oil compounds should remedy this disadvantage. The adsorption of essential oils onto a support such as clays is a technique that will immobilize volatile compounds, stabilize the essential oil and protect it against light, and modulate its release over time. Similar studies were done; montmorillonite and

kaolinite have been tested as effective materials for the adsorption of terpenic compounds, and the use of loaded clays as new natural insecticides has been proposed [13, 15, 16]; especially, the adsorption of thymol onto the purified bentonite and its counterpart modifies part CTAB [14].

In this context, we are interested in testing the affinity of thymol to Rhassoul by studying its adsorption kinetics to determine the relative adsorption capacity of each clay and specify the kinetic model and the adsorption isotherm.

## 2. Materials and Methods

*2.1. Raw Material.* The clay used in this study is from a commercial Rhassoul named "Rhassoul Chorafa Al Akhdar." It corresponds to the natural product crushed without any treatment and dried at 100°C to remove weakly bound water and then crushed and sieved. Only aggregates smaller than 63 $\mu$m in diameter were retained.

Thymol of 99% purity and sodium chloride (NaCl) of 98% purity were provided by Sigma-Aldrich; cetyltrimethylammonium bromide (CTAB) of 98% purity was provided by LOBA Chemie. NaOH and HCl were provided by Fisher.

*2.2. Purification of Rhassoul.* Rhassoul, previously crushed and sieved to a size less than 63 $\mu$m, is suspended in a solution of NaCl (1M concentration) to replace all the exchangeable cations ($Ca^{2+}$, $Mg^{2+}$, $K^{+}$,...) of the natural clay with the $Na^{+}$ ions. For this purpose, the mass $m$ of clay is introduced into a beaker containing 100 ml of an NaCl solution (1M). After 4 hours of stirring, the clay particles are separated from the aqueous phase by centrifugation at a speed of 3400 rpm/min during 10 min. After 4 successive treatments (saturation-centrifugation), the suspension is subsequently centrifuged and washed several times with distilled water until complete elimination of chloride ions (until the silver nitrate test is negative). The suspension obtained is dried at 70°C overnight, and the purified compound (Rh-P) is crushed using a porcelain mortar.

*2.3. Preparation of Rhassoul-CTAB (Rh-CTAB).* A suitable amount of cationic surfactant bromide, cetyltrimethylammonium bromide (CTAB), with purity >96% and the chemical formula $CH_3(CH_2)_{15}N(CH_3)_3^{+}\ Br^{-}$, was dissociated in distilled water previously heated to 40°C in order to increase the solubility of CTAB.

Rhassoul interposed by the surfactant cetyltrimethylammonium bromide (denoted Rh-CTAB) is obtained by dispersing 2.4 g of the Rh-P, decarbonated by HCl, and treated with $H_2O_2$ at 30% in 100 ml of distilled water (at a ratio of CTAB/Rhassoul equal to 1.14 mmol/g) to which a solution of cetyltrimethylammonium bromide (1 g of CTAB in 100 ml of distilled water) is added dropwise [10]. The mixture was stirred for 24 h, recovered by centrifugation, washed three times with distilled water, and dried at 60°C for 12 hours.

*2.4. Characterization Techniques.* The purified Rhassoul and modified one obtained were characterized by physicochemical techniques (XRD, FTIR, DTA/TGA, and SEM-EDX).

The X-ray diffraction analysis was carried out on powder using a Philips PW 1800 apparatus (K$\alpha$ copper line $\lambda = 1.5418$ Å, 40 kV, 20 mA). The spectra of the different samples were recorded in a $2\theta$ range between 1° and 80° with an angular increment of 0.02°. Infrared spectra were obtained using a Fourier transform spectrometer (FTIR) of Shimadzu IRAffinity-1S type. The samples were packaged as pellets with 12 mm diameter. The absorption spectra were recorded in the range of 400 to 4000 $cm^{-1}$ in absorbance with a resolution of 2 $cm^{-1}$. The textural was examined by the BET method using a Micromeritics ASAP 2010 device. The samples were degassed beforehand at 100°C under vacuum overnight. The DTA and TGA were carried out by using a Shimadzu TA-60 type apparatus operating under air with a linear heating rate of 10°C/min from room temperature up to 600°C. The morphology of the clay powder was observed using a scanning electron microscope TESCAN Vega3-EDAX instrument with an accelerating voltage of 20 kV. The elemental composition of our materials was determined by energy-dispersive X-ray spectroscopy (EDX).

*2.5. Methods.* Experiment adsorption was carried out in closed bottles protected from light. 20 ml of the aqueous solution of thymol, with an initial concentration of 80 mg/L, was brought into contact with 100 mg sample of Rhassoul. The adsorption kinetics of thymol on the different solids at room temperature was monitored at regular times (30 min, 1 h, 2 h, 4 h, 6 h, and 8 h) at a pH equal to 9. The mixture was passed through a filtration system with a 0.45 $\mu$m membrane before analysis. The filtrate was then analyzed by UV-visible spectroscopy, and the residual concentration was determined by measuring the absorbance at the wavelength of 273 nm.

The amount of thymol adsorbed (mg/g) was calculated using the following equation [17]:

$$q_e = \frac{(C_0 - C_e) \cdot V}{m}, \quad (1)$$

where $C_0$ and $C_e$ are, respectively, the initial and equilibrium concentrations of thymol in mg/L; $m$ is the mass of the adsorbent in g; $V$ is the volume of the thymol solution in mL; and $q_e$ is the amount adsorbed per gram of the adsorbent in mg/g.

The adsorption isotherms were carried out under the same conditions as those of the adsorption kinetics using the increasing concentration of thymol from 0 to 200 mg/L. The contents of the flasks were stirred for 5 hours until reaching the equilibrium time and then centrifuged. Residual concentrations and adsorbed quantities were determined as previously by (1).

## 3. Results and Discussion

*3.1. Characterization of Rhassoul*

*3.1.1. XRD Analysis.* The XRD patterns of raw Ghassoul clay ((a) in Figure 1) and the purified Rhassoul ((b) in Figure 1)

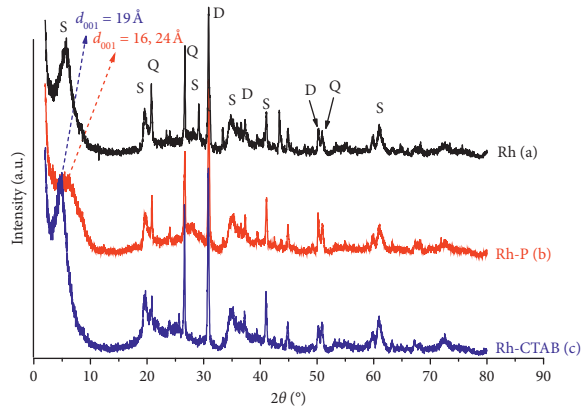


Figure 1: XRD patterns of Rh (a), Rh-P (b), and Rh-CTAB (c).

are similar, which shows that the dominant phase is stevensite with the presence of quartz and dolomite. The XRD patterns reveal the presence of the diffraction peak characteristic of stevensite (S) at $2\theta = 5.36^\circ$, $19.65^\circ$, $29.13^\circ$, $34.73^\circ$, $40.91^\circ$, and $60.6^\circ$ which is the majority phase of Rhassoul. The presence of the dolomite phase ($D$) is confirmed by the diffraction peak at $2\theta = 30.67^\circ$, $37.24^\circ$, and $50.18^\circ$. The quartz phase ($Q$) in small quantity as an impurity is manifested by the diffraction peak at $2\theta = 20.81^\circ$, $26.62^\circ$, and $50.95^\circ$. These results are similar to those reported previously by Benhammou et al. [18].

The diffractogram of Rhassoul modified with cetyltrimethylammonium bromide (CTAB) ((c) in Figure 1) reveals the displacement of the position of the diffraction peak (001) of stevensite towards the low values of $2\theta$. This shows an expansion of the Rhassoul interface space due to the insertion of the CTAB cationic surfactant. In Table 1, we give the positions in Å of the diffraction peak (001) for the starting compound and that treated by CTAB.

The baseline distance $d_{001}$ increases by 16.24 Å for the purified Rhassoul at 19 Å for the Rh-P intercalated by CTAB. This indicates that the increase in the spacing $d_{001}$ is attributed to the exchange of $Na^+$ by the cationic surfactant in the interspace.

*3.1.2. FTIR Analysis.* Figure 2 shows the infrared spectra of the two clays studied. The adsorption bands appearing in the 3700 to 3620 $cm^{-1}$ region correspond to the vibrations of the structural hydroxyl groups characteristic of the Rh-P and to the elongation vibrations of the OH group of the adsorbed water. The exact position of these bands and their intensities vary according to the nature of the molecule. They appear in the Rh-P at 3439 $cm^{-1}$ and the Rh-CTAB at 3416 $cm^{-1}$. The band corresponding to the stretching vibration of N–H groups appears around 3680 $cm^{-1}$, and those corresponding to the vibration of symmetrical and asymmetrical stretching of the C–H bond in $CH_2$ and $CH_3$ appear, respectively, at 2927 $cm^{-1}$ and 2855 $cm^{-1}$ (Figure 2(b)). The water molecules of the bending vibration of H–OH bands appear around 1632 $cm^{-1}$, while the bands characteristic of carbonates are detected in the purified and the modified Rhassoul at 1446 $cm^{-1}$, 1464 $cm^{-1}$, and 880 $cm^{-1}$. The characteristic bands of vibration deformation of the Si–O bond of quartz manifest at 676 $cm^{-1}$ and 468 $cm^{-1}$ for the purified Rhassoul and 672 $cm^{-1}$ and 471 $cm^{-1}$ for the modified one by CTAB. The infrared spectra of these solids also show the bands corresponding to the stretching vibration of the group Si–O–Si quartz at 1024 $cm^{-1}$ for both purified and modified clays.

Table 1: Basal distance of the diffraction peak (001) of the Rh-P and Rh-CTAB.

| Clay | $2\theta$ (°) | $d_{001}$ (Å) |
|---|---|---|
| Rh-P | 5.44 | 16.24 |
| Rh-CTAB | 4.65 | 19.00 |

The functions of the main vibration bands observed in the spectrum of the Rh-P and Rh-CTAB are shown in Table 2.

The results obtained by infrared are in good agreement with those revealed by X-ray diffraction. Both clays contain quartz.

*3.1.3. Scanning Electron Microscopy and Energy-Dispersive X-Ray Spectroscopy (SEM/EDX).* The SEM shows that the Rh-P ((a) in Figure 3) and Rh-CTAB ((a) in Figure 4) have an outer surface with more or less irregular form of platelets and heterogeneous structure ((a) in Figure 4).

On the contrary, the EDX spectrum of the Rh-P ((b) in Figure 3) shows the presence of chemical elements in the purified Rhassoul (Si, Al, Mg, Fe, K, P, S, O, and Ca). Table 3 shows a very high percentage of Si and Mg mainly due to the predominant presence of quartz and magnesium oxide in the clay studied [19]. These results confirm the validity of the X-ray diffraction analysis. The EDX spectrum of the Rh-CTAB ((b) in Figure 4) shows the presence of the same chemical elements as the purified Rhassoul with the appearance of the carbon element, which confirms the presence of the CTAB surfactant (Table 4) in agreement with the FTIR and the XRD which showed, respectively, the bands characteristics of C–H and N–H groups and a shift of the diffraction peak (001). The results of the analysis are summarized in Tables 3 and 4 for the two clays.

*3.1.4. DTA/TGA.* The DTA/TGA thermogram of the Rh-P (Figure 5) reveals the presence of an endothermic peak, with a maximum around 84°C, accompanied by a 7% loss of mass, which is attributed to the adsorbed water in the surface of the clay, and an exothermic peak whose maximum appears around 332°C accompanied by a loss of mass equal to 4% corresponding to the allotropic transformation of stevensite into enstatite [20].

The DTA/TGA thermogram of the Rh-CTAB (Figure 6) shows the presence of (i) an endothermic peak around 56°C with a weight loss of about 2%, which corresponds to the removal of water adsorbed on the surface, (ii) an endothermic peak around 290°C corresponding to the loss of the intercalated water molecules, and (iii) an exothermic peak whose maximum occurs at 346°C accompanied by a loss of mass equal to 20%, corresponding to the destruction of the cationic surfactant

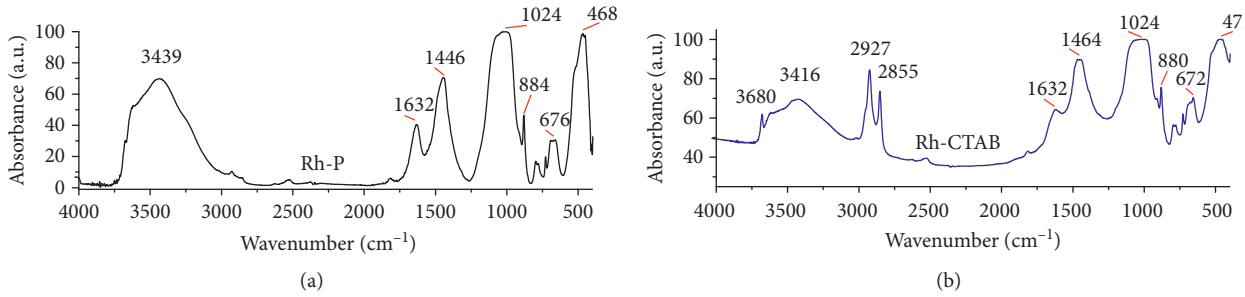


Figure 2: Infrared spectra of the Rh-P (a) and Rh-CTAB (b).

Table 2: Vibration bands of the Rh-P and Rh-CTAB.

| Vibration frequencies (cm$^{-1}$) | | Functions |
|---|---|---|
| Rh-P | Rh-CTAB | |
| — | 3680 | Stretching vibration of N–H groups |
| 3439 | 3416 | Stretching vibration of hydroxyl O–H |
| — | 2927 and 2855 | Symmetric and asymmetric stretching vibrations of C–H in $CH_2$ and $CH_3$ |
| 1632 | 1632 | Vibration deformation of the H–OH water molecules |
| 1446 | 1464 | Vibrations due to the presence of carbonates and C–H deformation vibration of Rhassoul modified |
| 1024 | 1024 | Stretching vibration of silica Si–O–Si |
| 884 | 880 | Bending vibration ($CO_3$) and $Al_2OH$ |
| 676 and 468 | 672 and 471 | Vibration deformation of Si–O–Si |

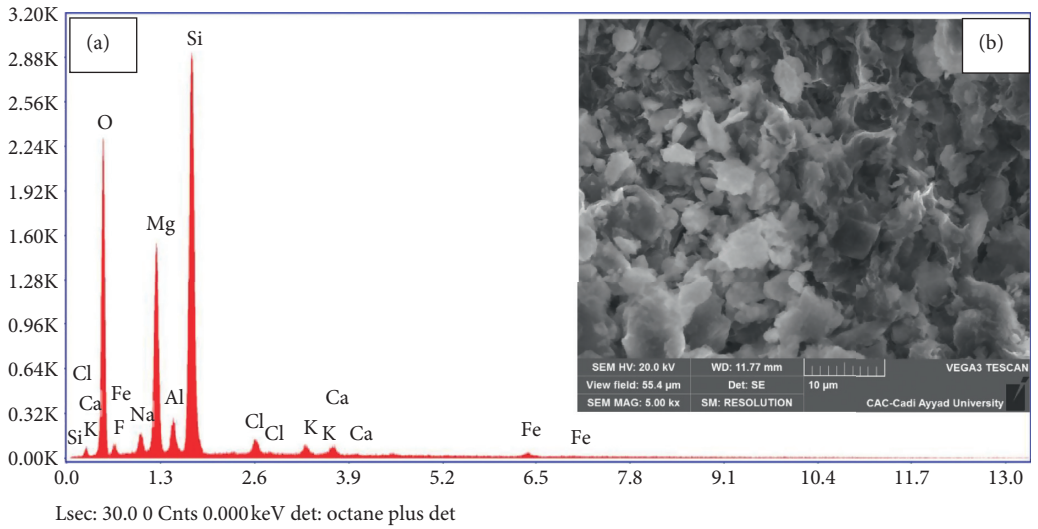


Figure 3: SEM-EDX micrograph of the Rh-P.

CTAB intercalated into the interlayer space and the allotropic transformation of stevensite into enstatite.

### 3.2. Adsorption Studies

*3.2.1. Adsorption Kinetics.* From Figure 7, it is seen that the adsorbed amount of thymol increases with contact time and equilibrium is reached near the end of 60 minutes for both the clays with a retention capacity $q_e \approx 16$ mg/g of the modified Rhassoul and $q_e \approx 6$ mg/g of the purified Rhassoul.

The curves represent the adsorption kinetics of thymol (Figure 7) makes it possible to highlight two phases; at first, the rapid and maximum adsorption is reached after about thirty minutes and corresponds to the external mass transfer. The second phase is slow and is related to the diffusion phenomenon as it has been obtained by Ziyat et al. in adsorption of thymol onto hydrotalcite Mg–Al–$CO_3$ [21]. This is related to the availability of free clay active sites at the beginning of the experiment and decreases gradually as we advance in time.

The results of the adsorption kinetics show that the amount of thymol adsorbed is greater for the Rh-CTAB compared to the Rh-P because the purified Rhassoul is initially hydrophilic and becomes organophilic after treatment with CTAB; subsequently, the affinity of the latter to

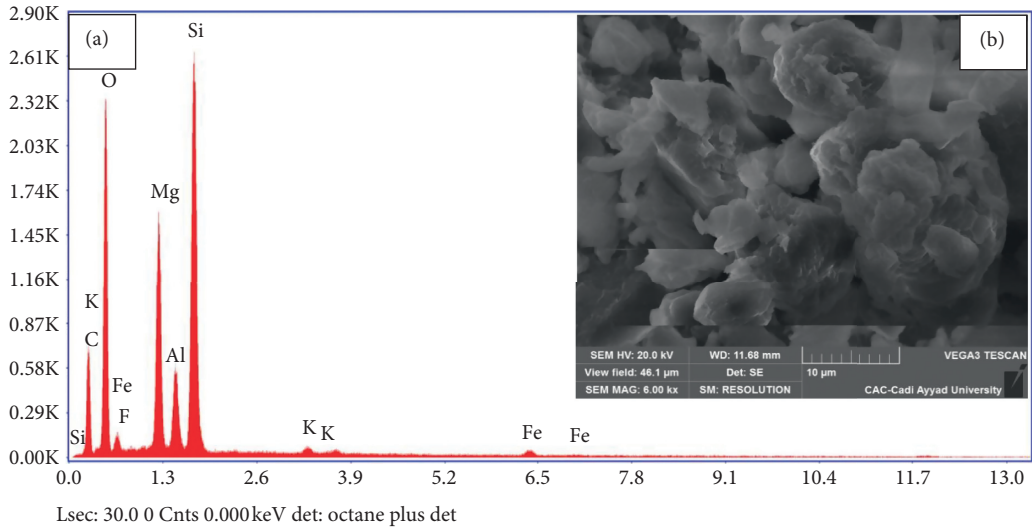


Figure 4: SEM-EDX micrograph of the Rh-CTAB.

Table 3: Chemical elements of the Rh-P in %.

| Elements | O | F | Na | Mg | Al | Si | Cl | K | Ca | Fe |
|---|---|---|---|---|---|---|---|---|---|---|
| Weight % | 44.6 | 2.7 | 2.0 | 14.9 | 2.4 | 29.4 | 1.3 | 0.8 | 1.0 | 0.9 |

Table 4: Chemical elements of the Rh-CTAB in %.

| Elements | C | O | F | Mg | Al | Si | K | Fe |
|---|---|---|---|---|---|---|---|---|
| Weight % | 27.7 | 39.9 | 3.6 | 9.2 | 3.6 | 14.6 | 0.4 | 0.9 |

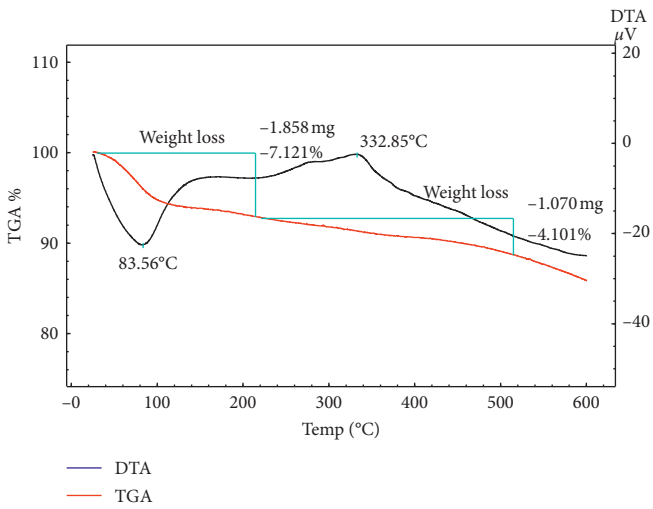


Figure 5: DTA/TGA thermogram of the Rh-P.

thymol increases, and the adsorbed quantity also increases. Similar results were obtained for Cr(VI) adsorption onto Al-montmorillonite and CTA-montmorillonite [22] and for Cr(VI) adsorption onto CTA-stevensite [10].

To understand the behavior of the adsorbent and examine the control mechanism of the adsorption process, the pseudo-first-order models, pseudo-second-order models,

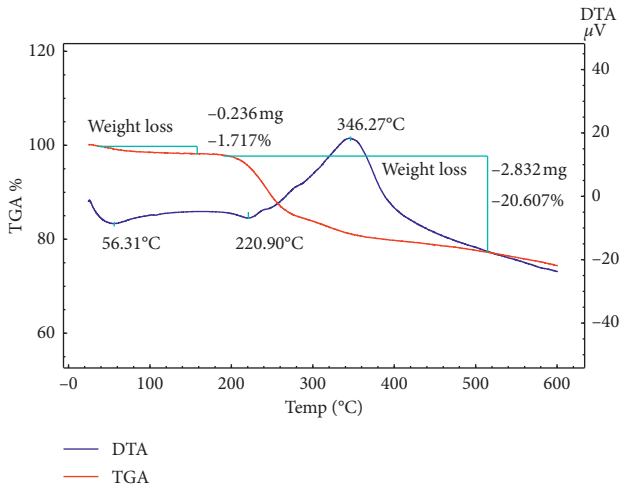


Figure 6: DTA/TGA thermogram of the Rh-CTAB.

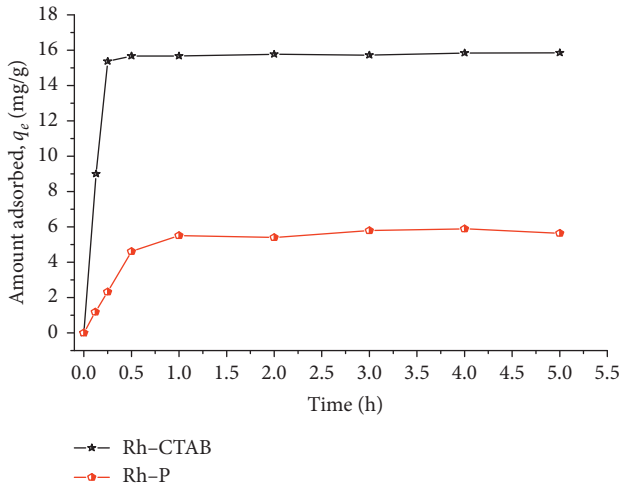


Figure 7: Adsorption kinetics of thymol onto the Rh-P and Rh-CTAB.

and intraparticle diffusion were applied to the experimental data.

The pseudo-first-order kinetic model [23–25] is given by

$$\ln(q_e - q_t) = \ln q_e - k_1 \cdot t, \quad (2)$$

where $q_e$ is the amount adsorbed at equilibrium per gram of the adsorbent (mg·g$^{-1}$), $q_t$ represents the quantity adsorbed at a given instant $t$ (mg·g$^{-1}$), $t$ is the contact time (min), and $k_1$ is the adsorption rate constant for the first order (min$^{-1}$). By plotting $\ln(q_e - q_t)$ versus the time $t$, the adsorption rate constant $k_1$ and the equilibrium adsorbed quantity $q_e$ can be determined.

The pseudo-second-order kinetic model [24, 26] is expressed as

$$\frac{t}{q_t} = \frac{1}{k_2 \cdot q_e^2} + \frac{t}{q_e}, \quad (3)$$

where $k_2$ is the adsorption rate constant for the pseudo-second-order (g·mg$^{-1}$·min$^{-1}$) and $q_e$ is the amount of the adsorbate at equilibrium per gram of the adsorbent (mg·g$^{-1}$).

The equilibrium adsorbed quantity ($q_e$) and the constant $k_2$ can be determined experimentally from the slope and ordinate at the origin of the line as $t/q_t$, a function of $t$.

It is noticed from Figure 8 that the pseudo-second-order model describes better the results of the adsorption of thymol onto the two clays. The adsorbed quantity values found in this model are very close to those determined experimentally (Table 5).

The values of the correlation coefficient $R^2$ of the second-order model are close to 1 ($R^2 \geq 0.99$) than those of the first-order model. The pseudo-second-order model is the most reliable for determining the order of adsorption kinetics of thymol on both clays and gives a better description of the adsorption kinetics compared to the pseudo-first-order model. This model was based on the assumption that the rate-limiting step might be chemical sorption or chemisorption involving valence forces through sharing or exchange of electrons between the adsorbent and the adsorbate [27, 28]. Similar results have been reported in the study of the adsorption of thymol onto clay-based adsorbents [14, 29], the adsorption of the basic yellow cationic dye onto Moroccan stevensite [5], and the adsorption of methyl violet onto rich clay stevensite from Morocco [6].

The intraparticle diffusion model proposed by Weber and Morris [30] is given by

$$q_t = k_d \cdot t^{1/2} + C, \quad (4)$$

where $k_d$ is the constant of intraparticle diffusion (mg·g$^{-1}$·h$^{-1/2}$) and $C$ is a constant which characterizes the diffusion of the solute in the liquid phase.

The plot of the adsorbed quantity $q_t$ versus $t^{1/2}$ shows two separate linear steps (Figure 9): a fast step at the beginning followed by a slow evolution towards the equilibrium state of adsorption for whatever adsorbent. The first step can be attributed to the external diffusion of the adsorbate to the surface of the adsorbent and the second step corresponds to the intraparticle diffusion due to the adsorbent-adsorbent interaction [31], confirming the results obtained from the pseudo-second-order kinetic model.

From Table 6, it is remarked that the values of $C$, the diffuse layer thickness constant, are different from 0, suggesting that intraparticle scattering is not the only factor controlling the adsorption rate of thymol on both clays. Wu et al. observed similar results in the study of the characteristics of the pseudo-second-order kinetic model for liquid-phase adsorption [32]. The surface properties including the number of adsorption sites also have an effect on the adsorption.

*3.2.2. Adsorption Isotherms.* The results of the study of thymol isothermal adsorption of the two samples are represented by the adsorbed amount based on the residual concentration of thymol. The obtained experimental isotherms are shown in Figure 10. These isotherms were compared with models of Langmuir and Freundlich, whose equations are given below.

Langmuir model [33]: it assumes that there is no interaction between the adsorbate molecules, and the maximum adsorption corresponds to the monolayer coverage given by

$$\frac{q_e}{q_{\max}} = \frac{(k_L \cdot C_e)}{(1 + k_L \cdot C_e)}. \quad (5)$$

The linear form of Langmuir (5) is

$$\frac{1}{q_e} = \frac{1}{C_e} \cdot \frac{1}{(q_{\max} \cdot K_L)} + \frac{1}{q_{\max}}, \quad (6)$$

where $q_e$ is the adsorbed amount at equilibrium (mg/g), $C_e$ is the equilibrium concentration (mg/L), $K_L$ is the equilibrium constant of Langmuir (L/mg), and $q_{\max}$ is the maximum adsorption amount (mg/g). The separation factor ($R_L$) is a dimensionless parameter whose expression is given by

$$R_L = \frac{1}{1 + K_L \cdot C_0}, \quad (7)$$

where $C_0$ is the initial concentration of the adsorbate (mg/L) and $K_L$ (L/mg) is the constant of Langmuir. When the separation factor ($R_L$) is between 0 and 1, the adsorption process is considered favorable [34, 35].

Freundlich model [36]: it is usually applied to the adsorption on heterogeneous solid surfaces it is represented by the following empirical formula:

$$q_e = k_F \cdot C_e^{1/n}. \quad (8)$$

The commonly used form is the linear form given by

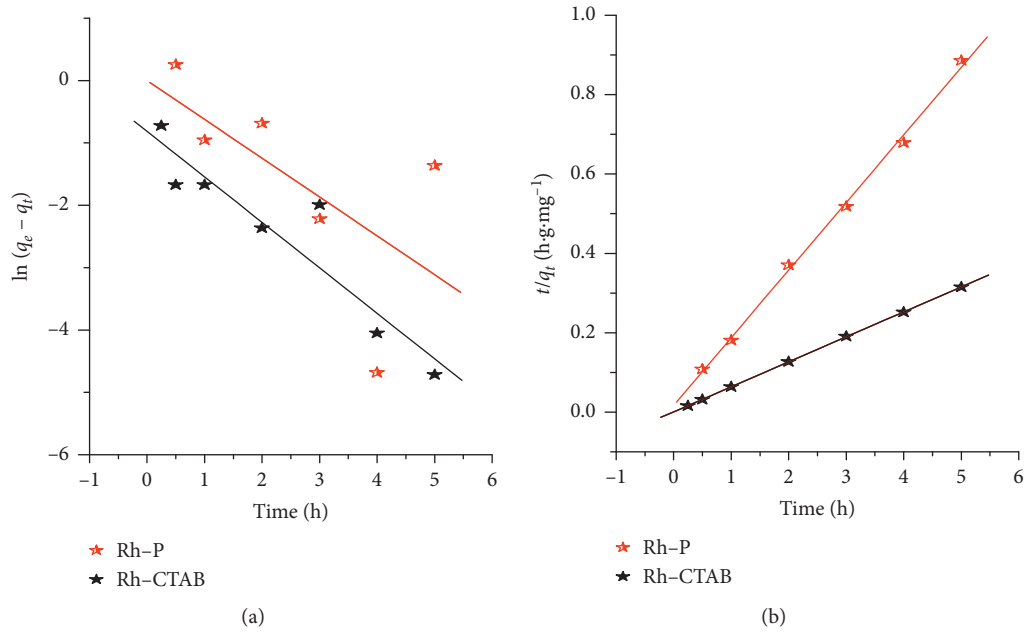


Figure 8: Linear representation of the kinetic model: (a) pseudo-first-order and (b) pseudo-second-order models for adsorption of thymol onto the Rh-P and Rh-CTAB.

Table 5: Pseudo-first-order and pseudo-second-order kinetic parameters for the adsorption of thymol onto the Rh-P and Rh-CTAB.

| | | Pseudo-first-order model | | | Pseudo-second-order model | | |
|---|---|---|---|---|---|---|---|
| Sample | $q_{exp}$ (mg/g) | $q_e$ (mg/g) | $K_1$ (h$^{-1}$) | $R^2$ | $q_e$ (mg/g) | $K_2$ (g·mg$^{-1}$·h$^{-1}$) | $R^2$ |
| Rh-P | 5.89 | 1.001 | 0.623 | 0.636 | 5.870 | 1.700 | 0.998 |
| Rh-CTAB | 15.85 | 0.443 | 0.730 | 0.935 | 15.891 | 4.747 | 0.999 |

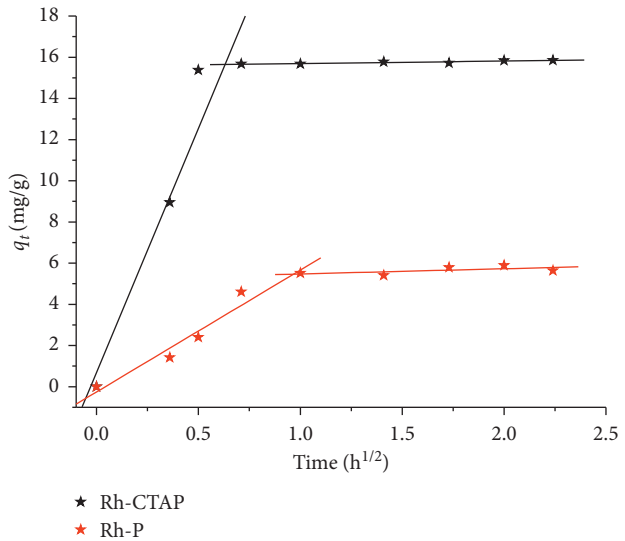


Figure 9: Model of intraparticle diffusion of thymol onto the Rh-P and Rh-CTAB.

Table 6: Intraparticle diffusion parameters of thymol onto the Rh-P and Rh-CTAB.

| | | 1st line | | | 2nd line | |
|---|---|---|---|---|---|---|
| Samples | $C$ | $K_{d1}$ (mg·g$^{-1}$·h$^{-1/2}$) | $R^2$ | $C$ | $K_{d2}$ (mg·g$^{-1}$·h$^{-1/2}$) | $R^2$ |
| Rh-P | 0.25 | 5.91 | 0.98 | 5.22 | 0.25 | 0.62 |
| Rh-CTAB | 0.7 | 23.69 | 0.96 | 15.57 | 0.12 | 0.90 |

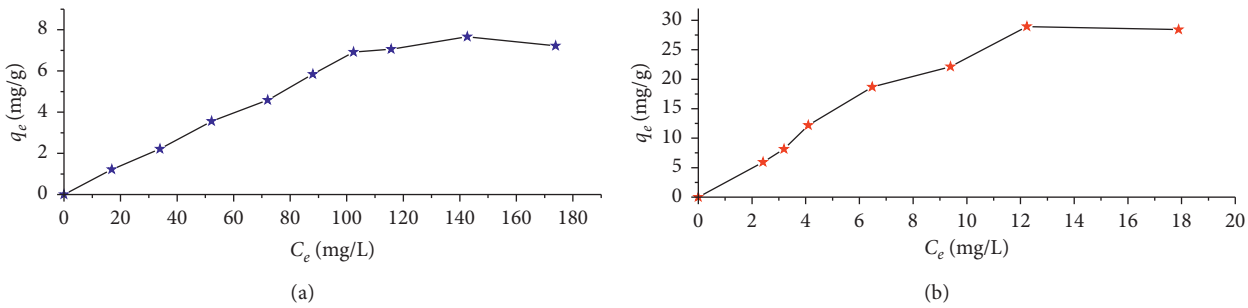


Figure 10: Adsorption isotherms of thymol onto the Rh-P (a) and Rh-CTAB (b).

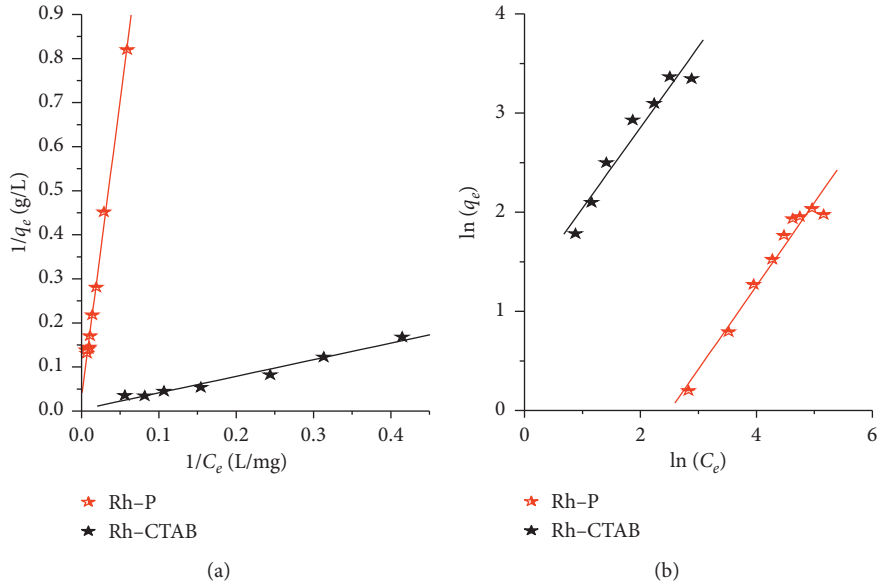


Figure 11: Linear representation of thymol adsorption isotherms onto the Rh-P and Rh-CTAB: Langmuir (a) and Freundlich (b).

Table 7: Langmuir and Freundlich fitting parameters for the adsorption of thymol onto the Rh-P and Rh-CTAB.

| Samples | Langmuir | | | | Freundlich | | |
|---|---|---|---|---|---|---|---|
| | $q_{max}$ (mg/g) | $K_L$ (mg/g) | $R_L$ | $R^2$ | $n$ | $K_F$ (mg g$^{-1}$) | $R^2$ |
| Rh-P | 31.221 | 0.0024 | 0.912–0.675 | 0.997 | 1.190 | 0.122 | 0.982 |
| Rh-CTAB | 277.01 | 0.010 | 0.33–0.714 | 0.986 | 1.228 | 3.404 | 0.970 |

$$\ln q_e = \ln K_F + \frac{1}{n}\ln C_e, \tag{9}$$

where $q_e$ is the concentration of the adsorbate (mg/g), often expressed in mg/L, $K_F$ is a constant of the adsorption capacity, and $n$ is a constant relative to the affinity between the adsorbate and the surface. The values of $n > 1$ represent favorable adsorption conditions [37].

The curves of linear transforms obtained by Langmuir and Freundlich models are shown in Figure 11, and different parameters of the two models are summarized in Table 7.

From the results of Table 7, it is remarked that the correlation coefficients $R^2$ of both models (Langmuir and Freundlich) show a good correlation with experimental data for both clays ($R^2 \geq 0.97$). However, the amounts adsorbed $q_{max}$ calculated from the Langmuir model are much different from those found experimentally for both clays, which means that the Langmuir model is not valid to describe the adsorption.

In addition, the values of $n$ from the Freundlich model (Table 7) are greater than 1 for both clays studied, indicating that the adsorption is favorable and the values of $K_F$ are large. Therefore, the Freundlich model is most likely to characterize the adsorption of thymol onto both adsorbents. Similar results have been observed for the adsorption of

thymol onto various adsorbents [14], for the removal of the basic yellow cationic dye by Moroccan stevensite [5], and for the adsorption of thymol onto hydrotalcite Mg–Al–$CO_3$ and onto its counterpart enabled at 500°C [21]. In conclusion, the model which adequately expresses the experimental data of the adsorption of thymol onto the two clays is that of Freundlich.

## 4. Conclusion

Interesting results are found in this study as follows.

Rhassoul used in this study has a majority stevensite phase characteristic of the clay from Morocco. This treated with CTAB has an expansion space interfolliaire, indicating the insertion of the surfactant as it was observed by XRD and FTIR. The study of the adsorption of thymol onto Rhassoul shows that there is affinity of thymol to Rhassoul. The results of the adsorption kinetics show that the adsorption of thymol onto the purified Rhassoul and modified one by CTAB is fast and the maximum quantity is reached after 40 min of adsorption. The modeling of the adsorption kinetics revealed its conformity to the pseudo-second-order model for the purified Rhassoul and also for its counterpart modified by CTAB. The experimental results are favorable for adsorption by the Freundlich model than by the Langmuir model for both clays. The modification of Rhassoul by CTAB greatly improves its adsorption capacity. It goes from almost 6 mg/g for the purified Rhassoul to a value of about 16 mg/g for the modified Rhassoul (Rh-CTAB).

## Data Availability

The authors confirm that all data underlying the findings of this study are fully available without restriction.

## Conflicts of Interest

The authors declare no conflicts of interest.

## Acknowledgments

This work was done in the framework of the project PPR2 supported by MENFPESRS and CNRST, Rabat, Morocco.

## References

[1] N. Trauth, *Argiles Évaporitiques Dans la Sédimentation Carbonateé Continentale et Épicontinentale Tertiaire*, Bassins de Paris, de Mormoiron et de Salinelles (France) et du Jbel Ghassoul (Maroc), Paris, France, 1974.

[2] S. Azarkan, A. Peña, K. Draoui, and C. I. Sainz-Díaz, "Adsorption of two fungicides on natural clays of Morocco," *Applied Clay Science*, vol. 123, pp. 37–46, 2016.

[3] K. Elass, A. Laachach, A. Alaoui, and M. Azzi, "Removal of methylene blue from aqueous solution using ghassoul, a low-cost adsorbent," *Applied Ecology and Environmental Research*, vol. 8, no. 2, pp. 153–163, 2010.

[4] Y. El Mouzdahir, A. Elmchaouri, R. Mahboub, A. Gil, and S. A. Korili, "Adsorption of methylene blue from aqueous solutions on a moroccan clay," *Journal of Chemical & Engineering Data*, vol. 52, no. 5, pp. 1621–1625, 2007.

[5] M. Ajbary, A. Santos, V. Morales-Flórez, and L. Esquivias, "Removal of basic yellow cationic dye by an aqueous dispersion of Moroccan stevensite," *Applied Clay Science*, vol. 80-81, pp. 46–51, 2013.

[6] K. Elass, A. Laachach, A. Alaoui, and M. Azzi, "Removal of methyl violet from aqueous solution using a stevensite-rich clay from Morocco," *Applied Clay Science*, vol. 54, no. 1, pp. 90–96, 2011.

[7] Y. El Mouzdahir, A. Elmchaouri, R. Mahboub et al., "Interaction of stevensite with $Cd^{2+}$ and $Pb^{2+}$ in aqueous dispersions," *Applied Clay Science*, vol. 35, no. 1-2, pp. 47–58, 2007.

[8] Y. Bentahar, C. Hurel, K. Draoui, S. Khairoun, and N. Marmier, "Adsorptive properties of Moroccan clays for the removal of arsenic (V) from aqueous solution," *Applied Clay Science*, vol. 119, pp. 385–392, 2016.

[9] L. Bouna, B. Rhouta, M. Amjoud et al., "Correlation between eletrokinetic mobility and ionic dyes adsorption of Moroccan stevensite," *Applied Clay Science*, vol. 48, no. 3, pp. 527–530, 2010.

[10] A. Benhammou, A. Yaacoubi, L. Nibou, and B. Tanouti, "Chromium (VI) adsorption from aqueous solution onto Moroccan Al-pillared and cationic surfactant stevensite," *Journal of Hazardous Materials*, vol. 140, no. 1-2, pp. 104–109, 2007.

[11] A. Benhammou, A. Yaacoubi, L. Nibou, and B. Tanouti, "Study of the removal of mercury(II) and chromium(VI) from aqueous solutions by Moroccan stevensite," *Journal of Hazardous Materials*, vol. 117, no. 2-3, pp. 243–249, 2005.

[12] Y. Li, A.-S. Fabiano-Tixier, and F. Chemat, "Essential oils: from conventional to green extraction," in *Essential Oils as Reagents in Green Chemistry*, pp. 9–21, Springer, Cham, Switzerland, 2014.

[13] M. M. G. Nguemtchouin, M. B. Ngassoum, L. S. T. Ngamo, X. Gaudu, and M. Cretin, "Insecticidal formulation based on *Xylopia aethiopica* essential oil and kaolinite clay for maize protection," *Crop Protection*, vol. 29, no. 9, pp. 985–991, 2010.

[14] M. G. M. Nguemtchouin, M. B. Ngassoum, R. Kamga et al., "Characterization of inorganic and organic clay modified materials: an approach for adsorption of an insecticidal terpenic compound," *Applied Clay Science*, vol. 104, pp. 110–118, 2015.

[15] L. A. Tapondjou, C. Adler, H. Bouda, and D. A. Fontem, "Efficacy of powder and essential oil from *Chenopodium ambrosioides* leaves as post-harvest grain protectants against six-stored product beetles," *Journal of Stored Products Research*, vol. 38, no. 4, pp. 395–402, 2002.

[16] M. M. G. Nguemtchouin, M. B. Ngassoum, L. S. T. Ngamo et al., "Adsorption of essential oil components of *Xylopia aethiopica* (Annonaceae) by kaolin from Wak, Adamawa province (Cameroon)," *Applied Clay Science*, vol. 44, no. 1-2, pp. 1–6, 2009.

[17] Y. Huang, X. Ma, G. Liang, and H. Yan, "Adsorption of phenol with modified rectorite from aqueous solution," *Chemical Engineering Journal*, vol. 141, no. 1-3, pp. 1–8, 2008.

[18] A. Benhammou, A. Yaacoubi, L. Nibou, and B. Tanouti, "Adsorption of metal ions onto Moroccan stevensite: kinetic and isotherm studies," *Journal of Colloid and Interface Science*, vol. 282, no. 2, pp. 320–326, 2005.

[19] A. Benhammou, *Valorisation de la stevensite du jbel rhassoul: application à l'adsorption des métaux lourds*, Ph.D. thesis, Cadi Ayyad University, Marrakesh, Morocco, 2005.

[20] G. T. Faust, K. J. Murata, and Stevensite, "Redefined as a member of the montmorillonite group," *American Mineralogist*, vol. 38, pp. 973–987, 1953.

[21] H. Ziyat, M. Naciri Bennani, H. Hajjaj, S. Mekdad, and O. Qabaqous, "Synthesis and characterization of crude hydrotalcite Mg-Al-$CO_3$: study of thymol adsorption," *Research on Chemical Intermediates*, vol. 44, no. 7, pp. 4163–4177, 2018.

[22] B. S. Krishna, D. S. R. Murty, and B. S. Jai Prakash, "Surfactant-modified clay as adsorbent for chromate," *Applied Clay Science*, vol. 20, no. 1-2, pp. 65–71, 2001.

[23] S. Lagergren, "Zur theories der sogenannten adsorption gelöster stoffe," *Kungliga Svenska Vetenskapsakademiens Handlingar*, vol. 4, pp. 1–39, 1898.

[24] Y. S. Ho and G. McKay, "Sorption of dye from aqueous solution by peat," *Chemical Engineering Journal*, vol. 70, no. 2, pp. 115–124, 1998.

[25] Y.-S. Ho, "Citation review of lagergren kinetic rate equation on adsorption reactions," *Scientometrics*, vol. 59, no. 1, pp. 171–177, 2004.

[26] Y. S. Ho and G. McKay, "Pseudo-second order model for sorption processes," *Process Biochemistry*, vol. 34, no. 5, pp. 451–465, 1999.

[27] F. Jia, Q. Wang, J. Wu, Y. Li, and S. Song, "Two-dimensional molybdenum disulfide as a superb adsorbent for removing $Hg^{2+}$ from water," *ACS Sustainable Chemistry & Engineering*, vol. 5, no. 8, pp. 7410–7419, 2017.

[28] Y. Ho and G. Mckay, "The kinetics of sorption of divalent metal ions onto sphagnum moss peat," *Water Research*, vol. 34, no. 3, pp. 735–742, 2000.

[29] M. EL Miz, S. Salhi, I. Chraibi, A. El Bachiri, M. Fauconnier, and A. Tahani, "Characterization and adsorption study of thymol on pillared bentonite," *The Journal of Physical Chemistry*, vol. 4, no. 2, pp. 98–116, 2013.

[30] J. C. Weber and W. J. Morris, "Kinetics of adsorption of carbon from solutions," *Journal of the Sanitary Engineering Division American Society*, vol. 89, pp. 31–63, 1963.

[31] G. Mckay, "The adsorption of dyestuffs from aqueous solutions using activated carbon: an external mass transfer and homogeneous surface diffusion model," *AIChE Journal*, vol. 31, no. 2, pp. 335–339, 1985.

[32] F.-C. Wu, R.-L. Tseng, S.-C. Huang, and R.-S. Juang, "Characteristics of pseudo-second-order kinetic model for liquid-phase adsorption: a mini-review," *Chemical Engineering Journal*, vol. 151, no. 1–3, pp. 1–9, 2009.

[33] I. Langmuir, "The adsorption of gases on plane surfaces of glass, mica and platinum," *Journal of the American Chemical Society*, vol. 40, no. 9, pp. 1361–1403, 1918.

[34] K. R. Hall, L. C. Eagleton, A. Acrivos, and T. Vermeulen, "Pore- and solid-diffusion kinetics in fixed-bed adsorption under constant-pattern conditions," *Industrial & Engineering Chemistry Fundamentals*, vol. 5, no. 2, pp. 212–223, 1966.

[35] W. Weber and R. K. Chakravorti, "Pore and solid diffusion models for fixed bed adsorbers," *American Institute of Chemical Engineers*, vol. 20, no. 2, pp. 229–238, 1974.

[36] Freundlich, "Over the adsorption in solution," *The Journal of Physical Chemistry*, vol. 57, pp. 385–470, 1906.

[37] L. Wang, J. Zhang, R. Zhao, C. Li, Y. Li, and C. Zhang, "Adsorption of basic dyes on activated carbon prepared from *Polygonum orientale* Linn: equilibrium, kinetic and thermodynamic studies," *Desalination*, vol. 254, no. 1–3, pp. 68–74, 2010.